

Article

Not peer-reviewed version

---

# Research on the Regulation of Field Emission Properties in $Ti_3C_2$ MXene/Carbon Nanotube Composite Films

---

[Yan Chen](#) and [Peng Liu](#) \*

Posted Date: 24 December 2025

doi: 10.20944/preprints202512.2153.v1

Keywords: field emission;  $Ti_3C_2$  (MXene); CNT



Preprints.org is a free multidisciplinary platform providing preprint service that is dedicated to making early versions of research outputs permanently available and citable. Preprints posted at Preprints.org appear in Web of Science, Crossref, Google Scholar, Scilit, Europe PMC.

Copyright: This open access article is published under a [Creative Commons CC BY 4.0 license](#), which permit the free download, distribution, and reuse, provided that the author and preprint are cited in any reuse.

Disclaimer/Publisher's Note: The statements, opinions, and data contained in all publications are solely those of the individual author(s) and contributor(s) and not of MDPI and/or the editor(s). MDPI and/or the editor(s) disclaim responsibility for any injury to people or property resulting from any ideas, methods, instructions, or products referred to in the content.

Article

# Research on the Regulation of Field Emission Properties in $Ti_3C_2$ MXene/Carbon Nanotube Composite Films

Yan Chen <sup>1</sup> and Peng Liu <sup>2,\*</sup>

<sup>1</sup> School of Physics and Electronic Information, Mianyang Teachers' College, Mianyang 621000, China

<sup>2</sup> Department of Physics, State Key Laboratory of Low-Dimensional Quantum Physics Tsinghua-Foxconn Nanotechnology Research Center, Tsinghua University, Beijing, China

\* Correspondence: Pengliu@tsinghua.edu.cn; Tel.: +86-10-62794280

## Abstract

The 2-D  $Ti_3C_2$  (MXene) materials have found applications in various fields, particularly as a candidate for field emission electron source when mixed with carbon nanotubes (CNTs) as the electron source material. In this study, a novel multilayer film structure utilizing  $Ti_3C_2$  (MXene) / CNTs and fabricate a unique field emitter device using these 2-D  $Ti_3C_2$  (MXene) / CNT materials have been presented. The material exhibits a tensile stress of 950 MPa and a low elongation at break of 8%. Specifically, utilizing the sharp edges of this material for emission, the field emission characteristics of  $Ti_3C_2$  (MXene) and  $Ti_3C_2$  (MXene) / CNT have been compared. The field emission characteristics of  $Ti_3C_2$  (MXene) and  $Ti_3C_2$  (MXene) / CNT have been compared. Measuring the current density is up to  $3.49 A \cdot cm^{-2}$  at an electric field of  $2.91 V \cdot \mu m^{-1}$ , It has low turn-on field ( $E_{on}$ )  $1.6 V \cdot \mu m^{-1}$ , and low threshold electric field ( $E_{th}$ )  $0.22 \mu A \cdot cm^{-2}$ . The field enhancement factor  $\beta$  of  $Ti_3C_2$  (MXene) / CNT is about 4.5 times more than pristine  $Ti_3C_2$  (MXene). Utilizing curved tip of  $Ti_3C_2$  (MXene) / CNT emission, the field emission current device slightly increases surround the vacuum degree from  $1.0 \times 10^{-3}$  Pa to  $4.7 \times 10^{-5}$ , and the current can be emitted steadily for a duration of 1 hour under the voltage of 723 V and vacuum level of  $1.0 \times 10^{-3}$  Pa. Those results provide that this kind of multilayer film  $Ti_3C_2$  (MXene) / CNT exhibits exceptional mechanical properties and can be easily shaped, particularly suit to fabricate vacuum electronic devices and other uses.

**Keywords:** field emission;  $Ti_3C_2$  (MXene); CNT

## 1. Introduction

2-D  $Ti_3C_2$  (MXene) materials have found applications in various fields [1,2], including energy storage, supercapacitors and batteries [3], biomedicine [4], catalysis [5], environmental detection and so on. However, the two-dimensional MXene material exhibits relatively low mechanical properties, including tensile strength and elongation, and is very vulnerable to moisture due to its hydrophilicity. In order to enhance its elasticity, researchers have successfully fabricated composited devices by combining MXene with other materials, such as carbon fiber, expanded graphite, graphene, and even CNT, all of which possess exceptional electrical conductivity and flexibility [6]. Such as Rajasmita Malik and his team used MXene composite polymer (EMA) s with a concentration of 10% to make an elastic electron storage device [7]. And mix graphene oxide or carbon nanotubes can be increase its strength and reduce infrared absorption [8,9]. Mengyao Xu and his team adopted the autocatalytic growth of CNTs on  $Ti_3C_2Tx$  nanosheets at low temperature and combined with the thermal annealing technology in nitrogen atmosphere to prepare a mixture of  $Ti_3C_2Tx$ -cnts [10]. As electromagnetic interference (EMI) shielding materials [11,12], Hao Wu's team used a natural rubber NR and combined it into a "sandwich" structure of a composite membrane of NR / MXene / CNTs to enhance its durability and thermoelectric conversion, as well as hydrophobic. Its mechanical strength

of multilayer NR / MXene / CNTs-50 has a tensile stress of 20.7 MPa and elongation at break of 123.2% [13].

The materials can also be used in microwave absorption (MA) materials [14,15]. but the electric field emission properties of their structures in lower vacuum are rarely studied. Here, we utilized the vacuum-assisted filtration system and employed to fabricate a multilayer film of  $Ti_3C_2$  (MXene) / CNT. The measurement techniques have been employed to analyze the properties of MXene materials, such as SEM, x-ray diffraction (XRD) [16], field emission scanning electron microscopy (FESEM).

The characteristics of electric field emission are affected by the surrounding atmosphere. By utilizing vacuum assistance, the device's emitter can be measured in a vacuum environment, which can reduce the work function of materials [17]. MXene exhibits high electrical conductivity values, such as metal-like electrical conductivity reaching  $\approx 20000 \text{ S}\cdot\text{cm}^{-1}$ , while nanotubes show semiconducting or metallic electronic properties. However, these materials are susceptible to sputter erosion and chemical contamination, which negatively impact their field emission behavior and result in degradation. Therefore, high vacuum conditions are necessary for operation [18].

Since 2020, Yan et al reported the utilization of 2D  $Ti_3C_2$  (MXene) as a cold field emission cathode material under the vacuum pressure of  $10^{-6}$  Pa. They achieved a measured current density of  $59 \text{ mA}\cdot\text{cm}^{-2}$  at an electric field strength of  $7.5 \text{ V}\cdot\mu\text{m}^{-1}$ . They further investigated the MXene– $TiO_2$  composite and measured an enhanced emission current density reaching up to  $289 \text{ mA}\cdot\text{cm}^{-2}$  from the cross-section of the composite film at a pressure of  $1.0 \times 10^{-5}$  Pa [19,20].

Based on previous study, Utilizing the sharp edge of this material for emission, a field emitter device using 2-D  $Ti_3C_2$  (MXene) material and  $Ti_3C_2$  (MXene) Mixing CNT have been fabricated respectively.

## 2. Experimental Section

### 2.1. Materials

The production of few-layer  $Ti_3C_2$  (MXene) can be achieved by utilizing various etchants and delamination techniques [21]. The wet-chemical etching methods commonly employed at the earliest stage involve the utilization of hydrofluoric acid (HF) or HF-containing solutions. the process can be represented by following equation:  $Ti_3AlC_2 + 3HF = Ti_3C_2 + AlF_3 + \frac{3}{2} H_2$  [22] [23] . Obviously , HF has more hazardous, In the current year,  $Ti_3AlC_2$  Mixture lithium fluoride (LiF) and concentrated hydrochloric acid (HCl) produced in situ HF to obtained  $Ti_3C_2$ . The delaminated solution of few-layer  $Ti_3C_2$  (MXene) was obtained using this method and purchased from Jilin 11 Technology Co., Ltd

The cross-stacked CNT films were fabricated using super-aligned carbon nanotubes. First, individual CNTs are extracted using tweezers. These individual tubes are then assembled into an initial ribbon without any interruptions. This initial thin ribbon is further extended to form a CNT film of the same width as the substrate. Finally, by stacking multiple layers of superaligned CNT films in a crosswise manner, a "cross-stack film" could be produced [24,25].

## 2.2. Preparation of $Ti_3C_2$ (MXene)/CNTs Films

A schematic illustration of the preparation process for the  $Ti_3C_2$  (MXene) / CNT film ( Figure 1), shows that the fabrication of  $Ti_3C_2$  (MXene) / CNT hybrid films involved a mixing filtration technique. Firstly, about 5 mg / ml aqueous solution  $Ti_3C_2$  (MXene) suspension was initially subjected to a 30-minute ultrasonic treatment as an initial step. The solutions should be subjected to vacuum filtration, with a volume of approximately 0.2ml each., a single layer  $Ti_3C_2$  (MXene) was deposited on the top of another CNT cross-stack film of four layers.and followed by vacuum-assisted filtration to complete a cycle. The process was repeated layer by layer ten times before finally unveiling the dried multilayer film.

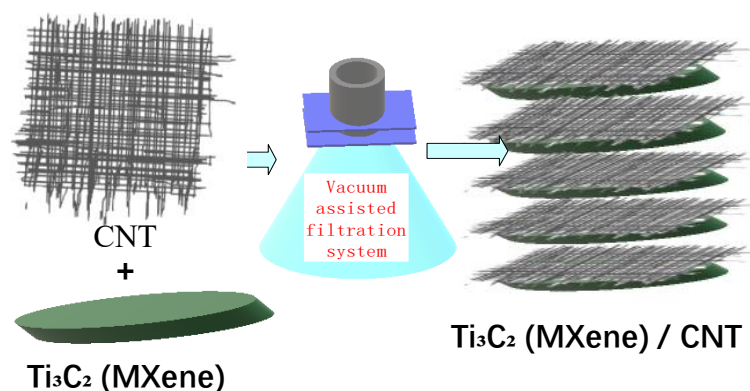


**Figure 1.** Schematic diagram for the fabrication of multilayer film  $Ti_3C_2$  (MXene)/CNT.

## 2.3. Fabrication of Emitters

The entire measurement the device process is conducted in vacuum atmosphere, utilizing a diode-type measurement system. The cathode is represented by a composite film measuring approximately 5 mm in length and 5 mm in width. A fluorescent screen is used as an anode, the distance (d) between the emitting surface and the anode is maintained at around 300  $\mu m$ .

## 3. Results and Discussion

### 3.1. Fabrication and Characterization of Film

The FESEM top view image of the film is shown (Figure 2a-d), with a voltage of 10KV applied, from image (Figure 2a,b) it can be observed that the surface morphology of film in pure  $Ti_3C_2$  (MXene) is predominantly flat, with a cross profile thickness of approximately 10  $\mu m$ . This structure provides an excellent emission source for subsequent cold field emission applications. Figure 2c,d. shows the surface and cross profile morphology after incorporating CNTs. It can be seen from the images that after doping CNT, the structures resemble spider webs. The stress–strain curves of  $Ti_3C_2$  (MXene) / CNT film have been described ( Figure2e), we can see that the film of  $Ti_3C_2$  (MXene) / CNT at a stretch speed of 0.1 mm / min, which has a high tensile stress of 950 MPa and a low elongation at break of 8%. The analysis reveals that the multilayer film of  $Ti_3C_2$  (MXene) / CNT exhibits fewer defects and demonstrates favorable tensile properties.

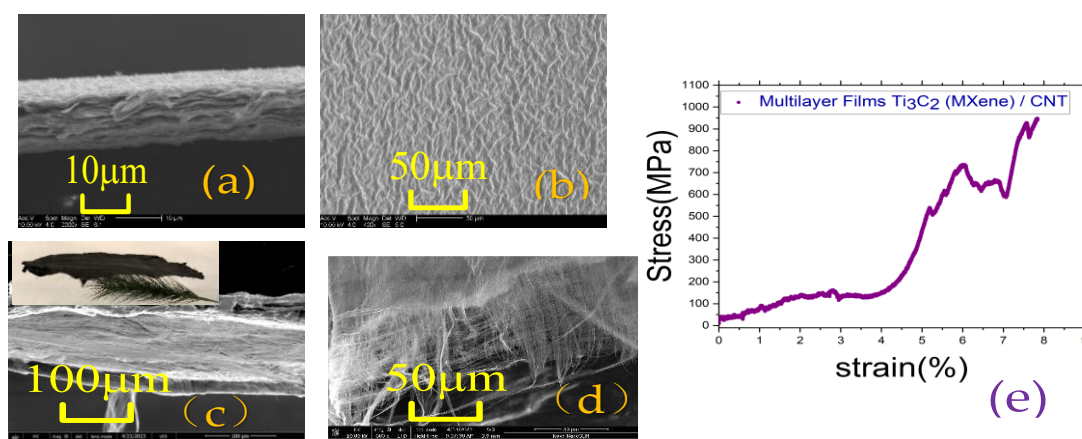


**Figure 2.** The SEM images of pristine  $\text{Ti}_3\text{C}_2(\text{MXene})$  film (a,b) and  $\text{Ti}_3\text{C}_2(\text{MXene})/\text{CNT}$  film (c,d) the stress-strain curves of  $\text{Ti}_3\text{C}_2(\text{MXene})/\text{CNT}$ (e).

### 3.2. Results and Discussion

The cross-section of the  $\text{Ti}_3\text{C}_2(\text{MXene})$  film was measured as a cold field emission cathode material. As depicted (Figure 3a, b) the results demonstrate that the current density can reach up to  $351 \text{ mA} \cdot \text{cm}^{-2}$  at an electric field of  $7.12 \text{ V} \cdot \mu\text{m}^{-1}$ , with a surrounding vacuum chamber pressure of  $3.7 \times 10^{-6} \text{ Pa}$ . Moreover, this device exhibits excellent current stability with minimal fluctuations over the course of one hour.

Analysis showed that Fowler-Nordheim from  $\text{Ti}_3\text{C}_2(\text{MXene})$  cathodes of the field electron emission. Figure 3c shows the typical Fowler-Nordheim plots under different vacuum chamber pressure, adopt cross-section of composite film. From the linear plots, it can be deduced that the electron emission process from  $\text{Ti}_3\text{C}_2(\text{MXene})$  is a typical Fowler-Nordheim tunneling behavior. In the linear zone, the slope of the straight line is similar to the same, that is to say, it has nearly no relation to vacuum degree.

The crystal structures of samples were determined using X-ray diffraction (XRD, Rigaku Smart Lab-SE, Japan) with  $\text{Cu-K}\alpha$  radiation (40 KV, 200 mA), and a scanning rate of  $4^\circ \text{min}^{-1}$  from  $5^\circ$  to  $85^\circ$ . The XRD patterns shown (Figure 3d) reveal that the  $\text{Ti}_3\text{C}_2(\text{MXene})$  crystals, As can be observed, the crystals exhibit prominent peaks at  $7.04^\circ$  (002), while the peak of (002) shifts towards smaller angles, indicating simultaneous intercalation and weakening. These results provide confirmation that the nanosheets have been successfully prepared. After mixing the CNT, the crystals peaks of  $\text{Ti}_3\text{C}_2(\text{MXene})$  are located  $6.7^\circ$ (002), indicating the crest creates a tiny amount of movement, The shift in crystal peaks indicates that the interlayer spacing increases after maximizing the CNT film [26]. The CNT peak of (002) is located  $25.27^\circ$ , and those peaks are narrow and sharp due to the high crystallinity. From Figure 4.b, the analysis reveals the presence of a crystalline peak in close proximity to the CNT (002) peak, observed at  $24.9^\circ$ , which corresponds to the formation of  $\text{TiO}_2$  during the hydrothermal reaction [13].

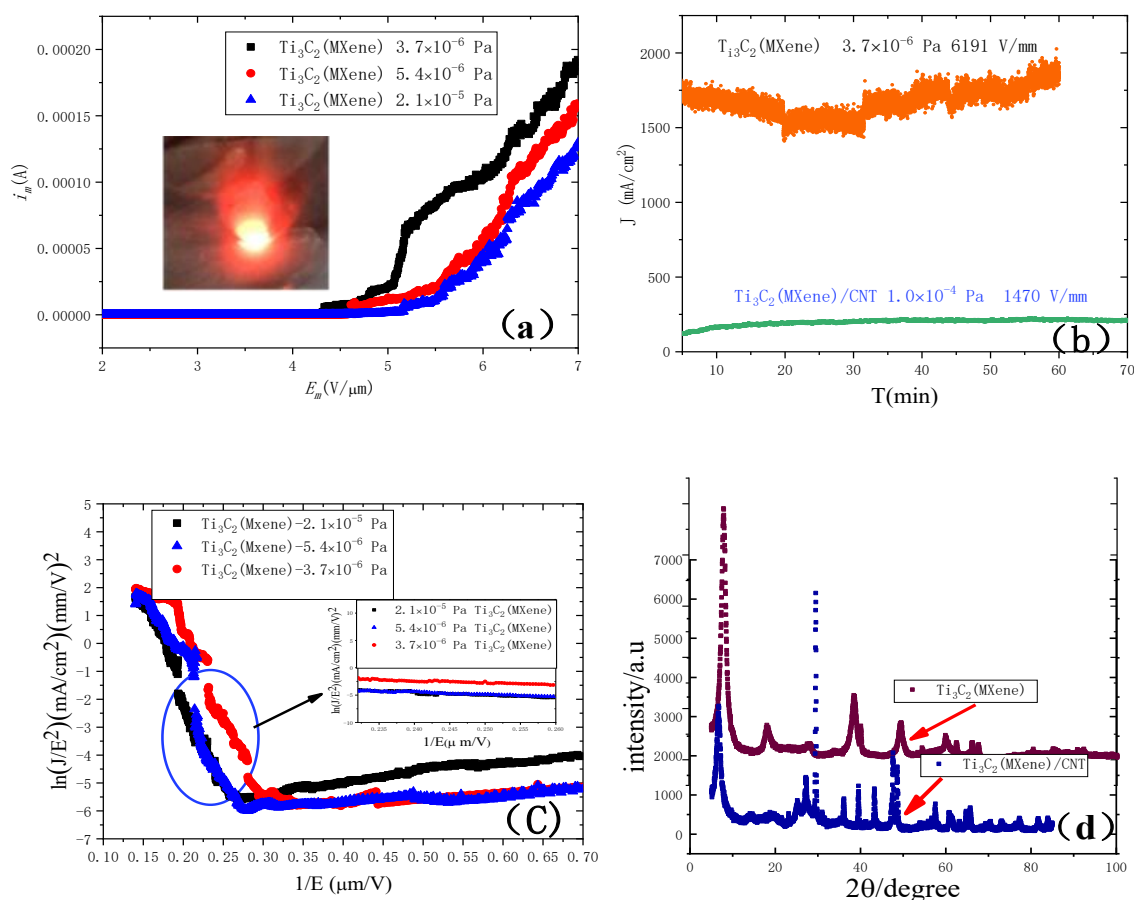


**Figure 3.** The J-E curve surround vacuum chamber pressure  $3.7 \times 10^{-6}$  Pa and  $2.1 \times 10^{-5}$  Pa . **(a)** The stability (J-t) curve current of field emission under the electric field intensity 6191V/ mm. **(b)** The typical Fowler-Nordheim plots under different vacuum pressure. **(c)** The XRD patterns combined with films of Ti<sub>3</sub>C<sub>2</sub>(MXene) and Ti<sub>3</sub>C<sub>2</sub>(MXene)/CNTs. **(d)**.

According to relevant reports, the Ti<sub>3</sub>C<sub>2</sub>(MXene) material probably contains O, OH, and F [22]. (Figure 4a, b) The elemental analysis of Ti<sub>3</sub>C<sub>2</sub>(MXene) and Ti<sub>3</sub>C<sub>2</sub>(MXene)/CNT respectively, From EDS chart (Figure 4a) shows the presence of C, Ti atom, but no OH in the film. And these spectra indicate the existence of O atom and a minor amount residues of F atom which can combine with C atom to form a-C:F nanostructures [27,28]. From EDS chart, (Figure 4b) shows the presence of C, Ti, F atom, there is not OH in the film as well. After mixing carbon nanotube, measurements were conducted on the Ti<sub>3</sub>C<sub>2</sub>(MXene)/CNT composite as the cathode field emission under pressure  $2.4 \times 10^{-4}$  Pa (Figure 4c). Results showed that at an electric field of  $2.91 \text{ V} \cdot \mu\text{m}^{-1}$ , the current density reached up to  $3.49 \text{ A} \cdot \text{cm}^{-2}$  with a current value of 1.81mA. The turn-on field ( $E_{on}$ )  $1.6 \text{ V} \cdot \mu\text{m}^{-1}$ . The threshold electric field, applied electric field for generating a current density of  $0.22 \mu\text{A} \cdot \text{cm}^{-2}$  [29].

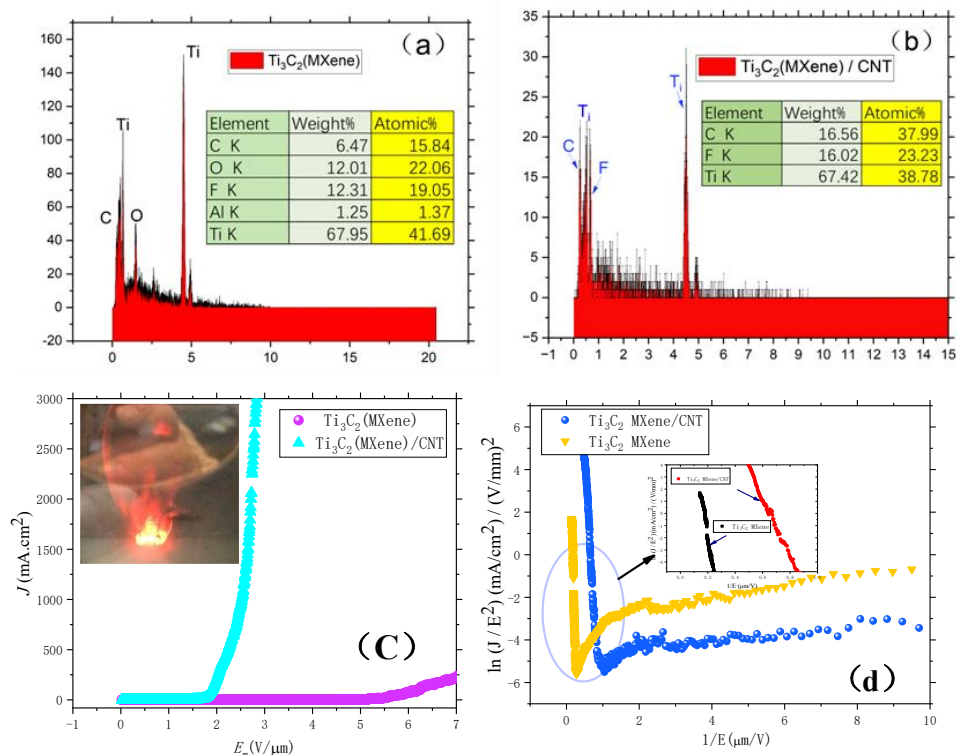


**Figure 4.** EDS spectra of  $Ti_3C_2(MXene)$  before (a) and after (b) field emission. The J-E curve field emission performance of  $Ti_3C_2(MXene) / CNT$ , and the surround vacuum pressure  $2.4 \times 10^{-4}$  Pa. (c) The typical Fowler-Nordheim plots under different vacuum pressure. (d).

From Figure 4d, the F-N plot displayed a straight line indicating that the electron has an excellent tunneling behavior. (Figure 4d) Display the shift of two materials before and after mixed the CNT, respectively. Based on the Fowler-Nordheim (F-N) theory, use the following equation:  $J = A\varphi^{-1}\beta^2 E^2 \exp\left(-\frac{B\varphi^{3/2}}{\beta E}\right)$  (mA·cm<sup>-2</sup>), transform it to the other equation:  $\ln\left(\frac{J}{E^2}\right) = \ln A \frac{\beta^2}{\varphi} - \frac{B\varphi^{3/2}}{\beta E}$ , where A and B is a constants, just depends on electron charge and its mass, and then  $A = 1.54 \times 10^{-6} A \cdot eV \cdot V^{-2}$  and  $B = 6.83 \times 10^9 v \cdot m^{-1} \cdot eV^{-3/2}$  respectively [30]. The parameter  $\varphi$  represents the work function of the cathode material [31]. The value of  $\beta$  can be calculated from the next the following equation:  $\beta = -\frac{B\varphi^{3/2}}{K}$ , here the parameter  $\beta$  is the field enhancement factor, and using the following value to calculate the field enhancement factor  $\beta$ .

Based on Thorsten Schultz and his co-workers calculation results. Use value of the work functions ( $\varphi$ ) of the  $Ti_3C_2(MXene)$  4.1 eV, to calculate the field enhancement factor  $\beta$  is 750 [32]. Moreover, combining the metallic CNTs with the dielectric  $Ti_3C_2(MXene)$ , use the  $\varphi = 4.8$  eV for the work function of CNT, the  $\beta$  of  $Ti_3C_2(MXene) / CNT$  is 3453. All the J-E curves (Figure 4c,d) of this study are satisfactorily fitted with the F-N equation [33]. By analyzing the slope of the linear portion (Figure 4d) using the F-N plot of  $\ln(J/E^2)$  versus  $1/E$ , we define this plot as parameter K [34–37]. It is evident that when  $Ti_3C_2(MXene)$  is mixed with CNT, the decrease in the plot can be attributed to either a reduction in the work function or an increase in the field factor ( $\beta$ ), and it may also result from their combination, and the other reason perhaps resulting Joule heating, which occur defect scattering on CNTs.

From the calculation, the field enhancement factor  $\beta$  present a different result. Firstly, the field enhancement factor  $\beta$  almost has nothing to do with the vacuum degree. From above Figure 4d, those devices of field emitter even though surround different vacuum environments, there are the same slope in the curves.

From Figure 3d, we can see that the XRD patterns films of  $\text{Ti}_3\text{C}_2$  (MXene) have a small amount  $\text{TiO}_2$ , this is own to consequence of oxidized, while Ti atoms exposed on the surface of  $\text{Ti}_3\text{C}_2$  (MXene) and also the oxygen elements in the environment, the Ti atoms easily can be oxidized into  $\text{TiO}_2$ . This is necessary a consequence of process, thus decreasing the conductivity of  $\text{Ti}_3\text{C}_2$  (MXene) [28,38], and this process as same as the material of  $\text{Ti}_3\text{C}_2$  (MXene) / CNTs. The band gap of  $\text{TiO}_2$  is 3.2 eV [16]. The work function  $\varphi$  of  $\text{TiO}_2$  is lower than  $\text{Ti}_3\text{C}_2$  (MXene), and calculate the field enhancement factor  $\beta$  must be low, coating  $\text{TiO}_2$  leading to transform the crystal structure and reduce the turn-on electric field and threshold electric field [29].

The significant affecting the field enhancement factor is the work function ( $\varphi$ ) of the emitting material. Using the relation  $\varphi = E_{\text{vac}} - E_{\text{F}}$ , here,  $E_{\text{vac}}$  is the electrostatic potential in the vacuum and  $E_{\text{F}}$  indicates the Fermi level [37]. After mixing the CNT, the  $\text{Ti}_3\text{C}_2$  (MXene) of field emission performance will be considerably enhanced, this may be due to electronic charge transfer results in the reduction of the work function.

And the surface resistivity is another influence factor under the electron emission from carbon films. This  $\text{Ti}_3\text{C}_2$  (MXene) structure due to addition of CNT, the conductive network can extend the current transmission path, so that the conductivity can be improved. The F-N curve reveals that for the same shape of the emitter, its field emission range remains linear and unaffected by changes in slope. Under identical external conditions, it can be inferred that the field enhancement factor remains constant. Furthermore, it has been observed that the value of  $\beta$  is strongly dependent on the device geometry, aspect ratio, aspect ratio (emitter geometry), screening effect, shape and size as will [39].

The film sample was subsequently transformed into a curved tip (with a central angle of approximately 45 degrees and a radius of about 10mm), replacing the original square shape. Utilizing tip emission. A fluorescent screen is used as an anode, the distance (d) between the emitting surface and the anode is maintained at around 500  $\mu\text{m}$ . We first tested the change of current with voltage in a low vacuum environment (about  $1.0 \times 10^{-3}$  Pa) and tested the stability, and then following using scanning electron microscopy to measurement the image of the emitted arc tip thin film material, Then increase the vacuum degree and repeat the experiment.

As depicted (Figure 5a,b) the field emission current of  $\text{Ti}_3\text{C}_2$  (MXene) / CNT device slightly increases with increasing vacuum degree, this phenomenon is attributed to the effects of vacuum environment on emission stability, current density and lifetime. In low vacuum conditions, ignition, gas ionization and ion bombardment cathode can occur and affect the performance of field emission devices. Conversely, high vacuum environments reduce gas molecule collisions and scattering between electrons and molecules while also decreasing the probability of gas adsorption by the chamber walls. These factors enhance electron emission from cathode materials leading to improved current stability.[17] Foretheremore, the brightness of the screen is also indicative of the size of the electron beam generated through field emission from the cathode material.

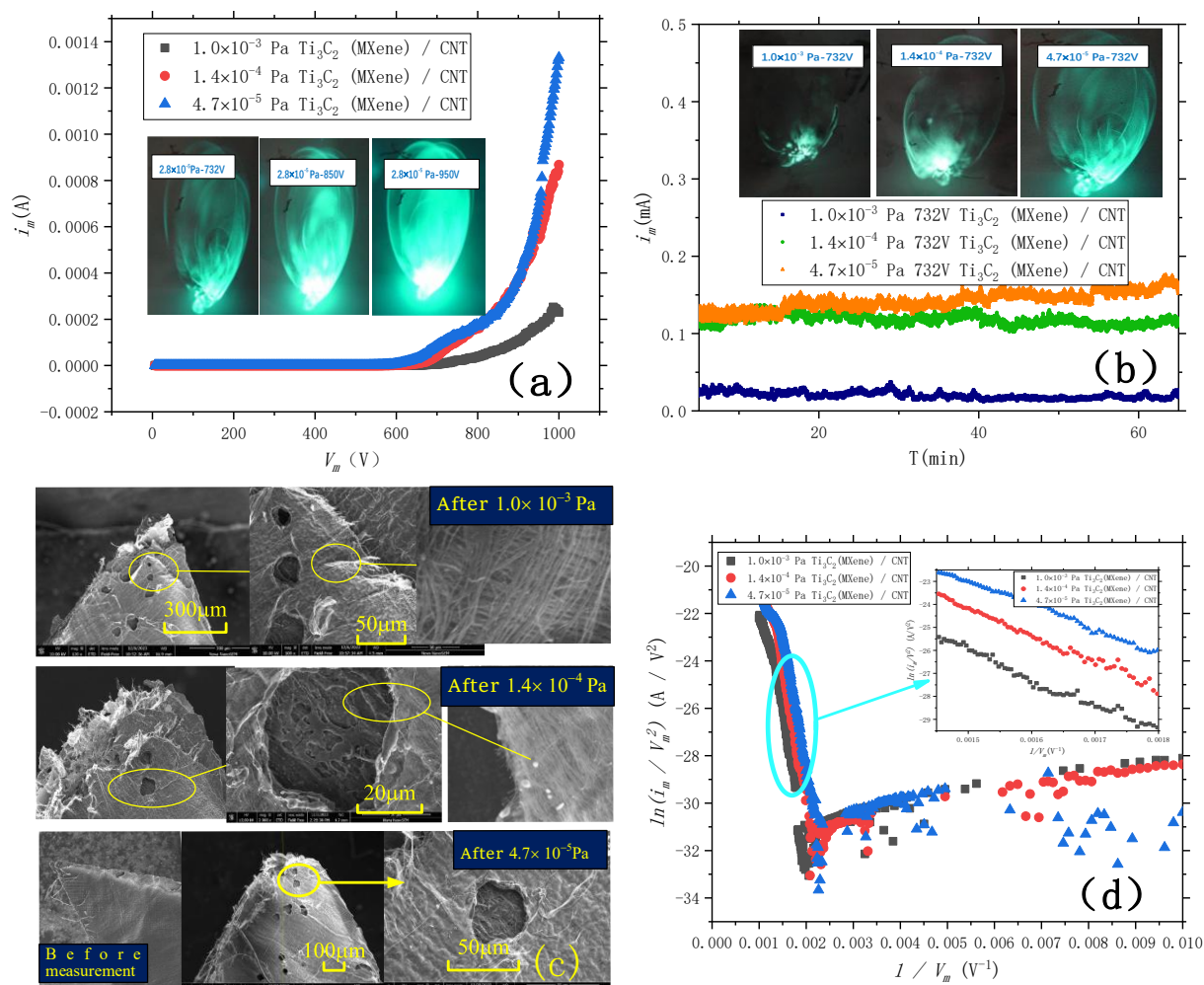


**Figure 5.** The I-V curve field emission performance of  $\text{Ti}_3\text{C}_2$  (MXene) / CNT (a) The typical Fowler-Nordheim plots under different vacuum pressure. (b) The SEM images of  $\text{Ti}_3\text{C}_2$  (MXene) / CNT film (c). The typical Fowler-Nordheim plots under different vacuum pressure (d).

The morphological changes observed after each test are depicted (Figure 5c), which shows SEM images of  $\text{Ti}_3\text{C}_2$  (MXene) / CNT film. It is evident that as the tests progress towards the tip, the sample experiences more severe damage. Following the initial low vacuum ( $1.0 \times 10^{-3}$  Pa) test, significant morphological alterations occurred, particularly at the posterior region of the tip where holes were observed. Additionally, it was apparent that CNT within the surface layer had undergone vaporization, potentially attributed to field emission under low vacuum conditions and thermal effects caused by emitted oxygen leading to carbon vaporization into holes on the surface. However, minimal damage was observed on lower regions due to their coverage by  $\text{Ti}_3\text{C}_2$  (MXene) film. This phenomenon can be explained by Joule-heating resulting from increased temperature, while the local carrier generation promoting that emission simultaneously enhancing. Furthermore, the nanochannels can be limit transportation of generated holes. The source material of the emission has remained relatively unchanged over an extended period of time, primarily due to its ability to inversely suppress net carrier generation and stabilize enhanced current flow. [40] The outermost layer of the material is coated with a CNT film, and the presence of these small holes may be attributed to defects in the crystal structure of the CNTs. Consequently, electron accumulation occurs at these holes place, and leading to an increase in material temperature and subsequent vaporization.

Figure 5d shows the results of the analysis the experimental data using the corrected form of the Fowler–Nordheim (FN) FE theory. The results also show that the material has better field emission performance [41,42].

## 4. Conclusions

The Ti<sub>3</sub>C<sub>2</sub> (MXene) / CNT composite structure exhibits robust mechanical properties and is easily cut, making it suitable for electronic devices in low vacuum. Additionally, it demonstrates excellent field emission properties under low vacuum conditions. After mixing CNT, at an electric field of 2.91 V·μm<sup>-1</sup>, current density reached up to 3.49 A.cm<sup>-2</sup>. It has low turn-on field (E<sub>on</sub>) 1.6 V·μm<sup>-1</sup>, and low threshold electric field (E<sub>th</sub>) 0.22 μA.cm<sup>-2</sup>. And the field enhancement factor β is 3453, it is about 4.5 times more than pristine Ti<sub>3</sub>C<sub>2</sub> (MXene) (β=750). These materials are suited to fabricate vacuum devices.

The cold electron emission from 2D Ti<sub>3</sub>C<sub>2</sub> (MXene) was comparatively studied with Ti<sub>3</sub>C<sub>2</sub> (MXene) / CNTs nanosheets. Moreover, the field emission current is influenced by various factors, including the vacuum level, aspect ratio of the emission film material, shape of the cathode emission surface, temperature, surface structure of the film, and impedance of the anode phosphor screen. Additionally, it can be considered to modify the band structure of the material through introducing impurity elements, and alter the work function and consequently adjust the emission current. The development of new Ti<sub>3</sub>C<sub>2</sub> (MXene) / CNTs composites also offers us additional possibilities for investigating field emission performance, which will be our next focus.

These films exhibited robust mechanical properties and were easily molded into desired shapes, and also exhibits superior field emission characteristics in low vacuum conditions, rendering it highly suitable for electronic devices operating under such environments. Additionally, Ti<sub>3</sub>C<sub>2</sub> (MXene) / CNTs composites doped with other elements can also be utilized as pressure sensors and bilateral brakes. Furthermore, since Jianli Wang and his colleagues employed CNT / MXenes nanospheres for the fabrication of lithium-sulfur batteries in 2019, CNT / MXenes have been consistently reported as a promising material for solar cells. Combined with Carbon nanotubes (CNT) can be utilized to fabricate diverse optoelectronic devices that are especially suitable for operation in vacuum environment [43–45]. It is anticipated that these films will find potential applications in future research studies.

**Author Contributions:** The author specially thanks J.X.Wang, J.T.Wang, L.L.Zhang, H.T.Yang, J.J.Sun, and S. S. Fan. He for help during the preparation of the manuscript.

**Funding:** This work has been financially supported by the National Key Research and Development Program of China (2024 YFA 1210601) from the Ministry of Science and Technology of China.

**Conflicts of Interest:** The authors declare no conflict of interest.

## References

1. Lipatov, A.; Alhabeab, M.; Lukatskaya, M. R.; Boson, A.; Gogotsi, Y.; Sinitskii, A. Effect of Synthesis on Quality, Electronic properties and environmental stability of individual monolayer Ti<sub>3</sub>C<sub>2</sub> MXene flakes. *Adv. Electron. Mater* **2016**, *2*, 1600255.
2. Khan, K.; Tareen, A. K.; Iqbal, M.; Hussain, I.; Mahmood, A.; Khan, U.; Khan, M. F.; Zhang, H.; Xie, Z. J. Recent advances in MXenes: a future of nanotechnologies. *J. Mater. Chem. A* **2023**, *11*, 19764–19811.
3. Wu, H.; Shen, S. Q.; Xu, X. Y.; Qiao, C. Y.; Chen, X. H.; Li, J.; Li, W. W.; Wei, O. Y. Facile fabrication and high field emission performance of 2-D Ti<sub>3</sub>C<sub>2</sub>T<sub>x</sub> MXene nanosheets for vacuum electronic devices. *IEEE Transactions on Electron Devices* **2020**, *67*, 5138–5143.
4. Naguib, M.; Barsoum, M. W.; Gogotsi, Y. Ten Years of Progress in the Synthesis and Development of MXenes. *Adv. Mater.* **2021**, *33*, 2103393.

5. She, Z. W.; Fredrickson, K. D.; Anasori, B.; Kibsgaard, J.; Strickler, A. L.; Lukatskaya, M. R.; Gogotsi, Y.; Jaramillo, T. F.; Vojvodic, A. Two-Dimensional Molybdenum Carbide (MXene) as an Efficient Electrocatalyst for Hydrogen Evolution. *ACS Energy Lett.* **2016**, *1*, 589–594.
6. Kiran N. U., Deore A. B., More M. A., Late D. J., Rout C. S., Mane P., Chakraborty B., Besra L., Chatterjee S. Comparative study of cold electron emission from 2D  $Ti_3C_2T_x$  MXene nanosheets with respect to its precursor  $Ti_3SiC_2$  MAXphase. *ACS Appl. Electron. Mater.* **2022**, *4*, 2656–2666.
7. Hong, X. D.; Zheng, H. R.; Liang, D. Enhanced field emission properties From plasma treated  $Ti_3C_2T_x$  (MXene) emitters. *Mater. Res. Express* **2020**, *7*, 115011.
8. Zhan, Y. G.; Lei, L.; Cao, Y. X.; Yang, Y. Y.; Wang, W. J.; Wang, J. F. High-strength, low infrared emission nonmetallic films for highly efficient Joule/solar heating, electromagnetic interference shielding and thermal camouflage. *Mater. Horiz* **2023**, *10*, 235–247.
9. Ding, W. J.; Liu, P.; Bai, Z. Z.; Wang, Y. Y.; Liu, G. Q.; Jiang, Q. L.; Jiang, F. X.; Liu, P. P.; Liu, C. G.; Xu, J. K. Constructing Layered MXene / CNTs Composite Film with 2D–3D Sandwich Structure for High Thermoelectric Performance. *Adv. Mater. Interfaces* **2020**, *7*, 2001340.
10. Xu, M. Y.; Liang, L.; Qi, J.; Wu, T. L.; Zhou, D.; Xiao, Z. B. Intralayered Ostwald Ripening-Induced Self-Catalyzed Growth of CNTs on MXene for Robust Lithium–Sulfur Batteries. *Small* **2021**, *17*, 2007446.
11. Wan, S.J.; Li, X.; Chen, Y.; Liu, N.; Du, Y.; Dou, S.X.; Jiang, L.; Cheng, Q. F. High-strength scalable MXene films through bridging-induced densification. *Science* **2021**, *374*, 96–99.
12. Weng, G.M.; Li, J. Y.; Mohamed Alhabe; Christopher Karpovich; Wang H; Jason Lipton; Kathleen Maleski; Jaemin Kong; Evyatar Shaulsky; Menachem Elimelech; Yury Gogotsi; André D. Taylor Layer-by-Layer Assembly of Cross-Functional Semi-transparent MXene-Carbon Nanotubes Composite Films for Next-Generation Electromagnetic Interference Shielding. *Adv. Funct. Mater.* **2018**, *28*, 1803360.
13. Wu, H.; Zhu, C. B.; Li, X. L.; Hu, X. P.; Xie, H.; Lu, X.; Qu, J.P. Layer-by-layer assembly of multifunctional NR / MXene / CNTs composite films with exceptional electromagnetic interference shielding performances and excellent mechanical properties. *Macromol. Rapid Commun.* **2022**, *43*, 2200387.
14. Aamir Iqbal; Pradeep Sambyal; Chong Min Koo 2D MXenes for electromagnetic shielding: A Review, *Adv. Funct. Mater.* **2020**, *30*, 2000883.
15. Wu, F. S.; Hu, P. Y.; Hu, F. Y.; Tian, Z. H.; Tang, J. W.; Zhang, P. G.; Pan, L.; Michel W. Barsoum; Cai, L. Z.; Sun, Z. M. Multifunctional MXene / C aerogels for enhanced microwave absorption and thermal insulation. *Nano-Micro Lett.* **2023**, *15*, 194.
16. Lee, J. S.; You, K. H.; Park, C. B.; Photoactive, H. Low bandgap  $TiO_2$  nanoparticles wrapped by graphene. *Adv. Mater.* **2012**, *24*, 1084–1088.
17. Liu, P. Super-aligned carbon nanotube neutralizers for aerospace. *nature reviews electrical engineering* **2024**, *1*, 73-74.
18. Evtukh, A.; Hartnagel, H.; Yilmazoglu, O.; Mimura, H.; Pavlidis, *Band Bending and Work Function*. D. Vacuum nanoelectronic devices: novel electron sources and applications; John Wiley & Sons: Chennai, India, **2015**; PP.105-107.
19. Chen, J. T.; Yang, B. G.; Lim, Y. D.; Duan, W. H.; Zhao, Y.; Tay, B. K.; Yan, X. B.  $Ti_3C_2$  (MXene) based field electron emitters. *Nanotechnology* **2020**, *31*, 285701.
20. Yang, B. G.; Chen, J. T.; Wu, X. N.; Liu, B.; Liu, L. Y.; Tang, Y.; Yan, X. B. Enhanced field emission performance of MXene– $TiO_2$  composite films. *Nanoscale* **2021**, *13*, 7622–7629.
21. Alhabe, M.; Maleski, K.; Anasori, B.; Lelyukh, P.; Clark, L.; Sin, Saleesha; Gogotsi, Y. Guidelines for Synthesis and processing of two-dimensional titanium carbide ( $Ti_3C_2T_x$  MXene ). *Chem. Mater.* **2017**, *29*, 7633–7644.
22. Naguib, M.; Kurtoglu, M.; Presser, V.; Lu, J.; Niu, J. J.; Min, H.; Hultman, L.; Gogotsi, Y.; Barsoum, M. W. Two-dimensional nanocrystals produced by exfoliation of  $Ti_3AlC_2$ . *Adv. Mater.* **2011**, *23*, 4248–4253.
23. Shahzad, F.; Alhabe, M.; Hatter, C. B.; Anasori, B.; Hong, S. M.; Koo, C. M.; Gogotsi, Y. Electromagnetic interference shielding with 2D transition metal carbides (MXenes). *Science* **2016**, *353*, 1137-1140.
24. Yu, W.; Liu, C. H.; Fan, S. S. Advances of CNT-based systems in thermal management. *Nano Res.* **2021**, *14*, 2471–2490.

25. Jiang, K. L.; Wang, J. P.; Li, Q. Q.; Liu, L.; Liu, C. H.; Fan, S. S. Superaligned carbon nanotube arrays, films, and yarns: a road to applications. *Adv. Mater.* **2011**, *23*, 1154–1161.
26. Wang, Y. F.; Liang, L. Y.; Du, Z. R.; Wang, Y. M.; Liu, C. T.; Shen, C. Y. Biodegradable PLA / CNTs / Ti<sub>3</sub>C<sub>2</sub>T<sub>x</sub> MXene nanocomposites for efficient electromagnetic interference shielding. *J Mater Sci: Mater Electron* **2021**, *32*, 25952–25962.
27. Lai, S. H.; Chang, K. L.; Shih, H. C.; Huang, K. P.; Lin, P. Electron field emission from various morphologies of fluorinated amorphous carbon nanostructures. *Appl. Phys. Lett.* **2004**, *85*, 6248–6250.
28. Qiao, C. Y.; Wu, H.; Xu, X.; Guan, Z. X.; Ou-Yang, W. Electrical conductivity enhancement and electronic applications of 2D Ti<sub>3</sub>C<sub>2</sub>T<sub>x</sub> MXene materials. *Adv. Mater. Interfaces* **2021**, *8*, 2100903.
29. Pandey, A.; Prasad, A.; Moscatello, J. P.; Engelhard, M.; Wang, C. M.; Yap, Y. K. Very stable electron field emission from strontium titanate coated carbon nanotube matrices with low emission thresholds. *Pandeyetal* **2013**, *7*, 117–125.
30. De Rose, L. B.; Catanzaro, D. H.; Choi, C.; Scherer, A. Effect of praseodymium coating on electron emission from a nanoscale gold field emitter array. *J. Vac. Sci. Technol. B* **2023**, *41*, 042801.
31. Kuttel, O.M.; Groning, O.; Emmenegger, C.; Nilsson, L.; Maillard, E.; Diederich, L.; Schlapbach, L. Enhanced field emission from a carbon nanotube array coated with a hexagonal boron nitride thin film. *small* **2015**, *11*, 3710–3716.
32. Schultz, T.; Frey, N.C.; Hantanasirisaku, K.; Park, S.; May, S. J.; Shenoy, V. B.; Gogotsi, Y.; Koch, N. Surface Termination Dependent Work Function and Electronic Properties of Ti<sub>3</sub>C<sub>2</sub>T<sub>x</sub> MXene. *Chem. Mater.* **2019**, *31*, 6590–6597.
33. Ahmed, S. F.; Moon, M. W.; Lee, K. R. Enhancement of electron field emission property with silver incorporation into diamondlike carbon matrix. *Appl. Phys. Lett.* **2008**, *92*, 193502.
34. Jonge, N. D.; Allieux, M.; Doytcheva, M.; Kaiser, M.; Teo, K. B. K.; Lacerda, R. G.; Milne, W. I. Characterization of the field emission properties of individual thin carbon nanotubes. *Appl. Phys. Lett.* **2004**, *85*, 1607–1609.
35. Wu, Y. H.; Li, J.; Ye, J. C.; Song, Y. J.; Chen, X. H.; Huang, S. M.; Sun, Z.; Wei, O. Y. Outstanding field emission properties of titanium dioxide / carbon nanotube composite cathodes on 3D nickel foam. *Journal of Alloys and Compounds* **2017**, *726*, 675–679.
36. Forbes, R. G. Field emission: Applying the “magic emitter” validity test to a recent paper, and related research-literature integrity issues. *J. Vac. Sci. Technol. B* **2023**, *41*, 042807.
37. Mahajan, A.; Khan, N.; Yadav, K. K.; Jha, M.; Ghosh, S. Efficient field emission from ultrafine nanostructured lanthanum sulfide synthesized by chemical route. *App. Sur. Sci.* **2023**, *623*, 156996.
38. Limbu, T. B.; Chitara, B.; Orlando, J. D.; Garcia Cervantes, M. Y.; Kumari, S.; Li, Q.; Tang, Y. G.; Yan, F. Green synthesis of reduced Ti<sub>3</sub>C<sub>2</sub>T<sub>x</sub> MXene nanosheets with enhanced conductivity, oxidation stability, and SERS activity. *J. Mater. Chem. C* **2020**, *8*, 4722–4731.
39. Ahmed, sk. F.; Ghosh, P. K.; Khan, S.; Mitra, M. K.; Chattopadhyay, K. K. Low-macroscopic field emission from nanocrystalline Al doped SnO<sub>2</sub> thin films synthesized by sol–gel technique. *Appl. Phys. A* **2007**, *86*, 139–143.
40. Huang, Y. F.; Chen, Y.; Huang, Z. J.; Zeng, M. X.; Gu, Z. G.; Yang, W.; Chen, J. P-type Si-Tips with integrated nanochannels for stable nonsaturated high current density field electron emission. Personal use is permitted, but republication/redistribution requires IEEE permission. *Ieee transactions on electron devices* **2022**, *69*, 7, 3908–3913.
41. Hong, X. D.; Zheng, H. R.; Liang, D. Enhanced field emission properties from plasma treated Ti<sub>3</sub>C<sub>2</sub>T<sub>x</sub> (MXene) emitters. *Mater. Res. Express* **2020**, *7*, 115011.
42. Forbes, R. G.; Deane, J. H. B. Reformulation of the standard theory of Fowler–Nordheim tunnelling and cold field electron emission. *Proc. R. Soc., Ser. A* **2007**, *463*, 2907–2927.
43. Li, H. Q.; Wu, Z.; Xing, Y. Q.; Li, B. G.; Liu, L. Photoelectric synergistic response properties of the Ti<sub>3</sub>C<sub>2</sub>T<sub>x</sub> MXene - CNT / PDMS bilayer actuator. *Nano Energy.* **2022**, *103*, 107821.
44. Wang, J. L.; Zhang, Z.; Yan, X. F.; Zhang, S. L.; Wu, Z. H.; Zhuang, Z. H.; Han, W. Q. Rational design of porous N-Ti<sub>3</sub>C<sub>2</sub> MXene / CNT microspheres for high cycling stability in Li–S battery, *Nano-Micro Lett.* **2020**, *12*, 4.

45. Agresti, A.; Pazniak, A.; Pescetelli, S.; Vito, A. Di.; Rossi, D.; Pecchia, A.; Auf der Maur, M.; Liedl, A.; Larciprete, R.; Kuznetsov, D.V.; D. Saranin; Carlo, A. Di. Titanium-carbide MXenes for work function and interface engineering in perovskite solar cells. *Nat. Mater.* **2019**, *18*, 1228–1234.
46. Zhang, P. C.; Ru, X. H.; Li, H. Y.; Liang, H. Y.; Wang, H. P.; Yang, C. H.; Zhang, X. G.; Liu, Z. G.; Zhang, Q. Y.; Chen, Y. H. Efficient MXene / CNT electromagnetic shielding composite films with self-assembly multilayer structure. *J Mater Sci Mater Electron* **2023**, *34*, 39.

**Disclaimer/Publisher's Note:** The statements, opinions and data contained in all publications are solely those of the individual author(s) and contributor(s) and not of MDPI and/or the editor(s). MDPI and/or the editor(s) disclaim responsibility for any injury to people or property resulting from any ideas, methods, instructions or products referred to in the content.